Engineering Notes

ENGINEERING NOTES are short manuscripts describing new developments or important results of a preliminary nature. These Notes cannot exceed 6 manuscript pages and 3 figures; a page of text may be substituted for a figure and vice versa. After informal review by the editors, they may be published within a few months of the date of receipt. Style requirements are the same as for regular contributions (see inside back cover).

Analysis of Air Backflow and Pressurization Characteristics in the Nuclear Exhaust System Duct

B. Misra,* R. S. Fairall,† and B. Mandell‡
Aerojet-General Corporation, Sacramento, Calif.

Nomenclature

A = cross-sectional area of resonator, ft²
C = compliance, Eq. (5), lb-ft²/lbf
D = diameter, ft
F = force, lbf
f = friction factor
g_c = Newton's conversion constant, ft-lbm/lbf-sec²
K = effective bulk modulus, psf
K_c, K_e = contraction and entrance coefficients, respectively
L = length of resonator, ft; or inductance, Eq. (3), lbf-sec²/-lbm-ft²
M = molecular weight, lbm/mole
$m, \dot{m}$ = mass, lbm; and mass flow, lbm/sec
P_1 = engine test compartment (ETC) pressure, psia
P_c = chamber pressure, psia
P_{sc} = steam generator system (SGS) pressure, psia
R = resistance, lbf-sec/lbm-ft²
r = gas constant, ft-lbf/lbm-°R
T = temperature of gas, °R
t = time, sec
U = velocity, fps, or a unit step
V = ETC volume, ft³
W_s = steam flow rate, lbm/sec
W_p = purge gas flow rate, lbm/sec
W_{sd} = flow rate in secondary duct, lbm/sec
α = damping, constant, Eq. (11), sec
γ = initial pressure, psia
ρ = density, lbm/ft³
μ = viscosity, lbm/sec/ft

Introduction

GROUND-TESTING of a nuclear rocket engine in the downward firing position imposes strict design requirements on the ejector system that must turn the exhaust gases by 90° and emit them at a suitable exit plane. For the NERVA engine testing, these requirements are even more severe because the exhaust gas is hot hydrogen. Based on extensive analytical studies and scale-model tests, the nuclear exhaust system (NES) duct has been built. During testing to evaluate the performance characteristics of the duct, under simulated operating conditions, air backflow was observed if the steam generator system (SGS) failed when there was no nozzle gas or when the gas flow was below a certain level. An intrusion into the NES duct is not permissible, as the engine test compartment (ETC) contains hot H_2 during engine testing. Also, excess pressure above the ambient pressure in the ETC could occur because of sudden pressurization resulting from the failure of the secondary fluid system. Such overpressurization may exceed the structural integrity of the ETC.

The major components (see Fig. 1) of interest here are the ETC and the shields that provide an inert atmosphere and radiation shield during engine testing, the NES, which provides limited altitude simulation (7–8 psia) within the ETC by the aerodynamic pumping action of the exhaust gases, and the SGS, which produces steam (130 psia and 1400°R) that is injected into duct through downstream-oriented nozzles.

The problem associated with the malfunction of either the primary or the secondary gas may be explained by means of the equilibrium relationship between the ETC pressure P_1, the nozzle chamber pressure P_c, and the secondary fluid pressure P_{sc}, as represented in Fig. 2. Below the duct pull-in (full-flow) point C a malfunction in the SGS, for example, at point A will result in repressurization of the cell from point A to point B. If the change of fluid mass in the ETC during this interval exceeds the combined flow of the primary and the secondary fluids, then air intrusion into the ETC will occur.

A simplified one-dimensional approach to the complex flow problem was made, based on mass balance, to define the gross behavior of the system and to identify the conditions under which air backflow occurs. Similarly, the repressurization characteristics (frequency and amplitude of pressure oscillations) of the ETC were analyzed by using linear network theory based on a two-node repressurization of the duct.

Air Intrusion

In the absence of primary gas flow, a mass balance for the ETC and the NES duct yields

$$(V_1 M_1/rT_1)dP_1/dt = W_p + W_S - W_{SD} \qquad (1)$$

From the experimental values of T_1 and dP_1/dt, the rate of change of mass in the cell was calculated and compared with the combined flow rates of steam and purge gas, $W_P + W_S$. When the rate of change of mass in the cell was larger than $W_P + W_S$, it was concluded that air must enter the cell to satisfy the equation of conservation of mass. Thus, from a simple mass balance, the amount of air that will enter the duct under a given set of operating conditions can be deter-

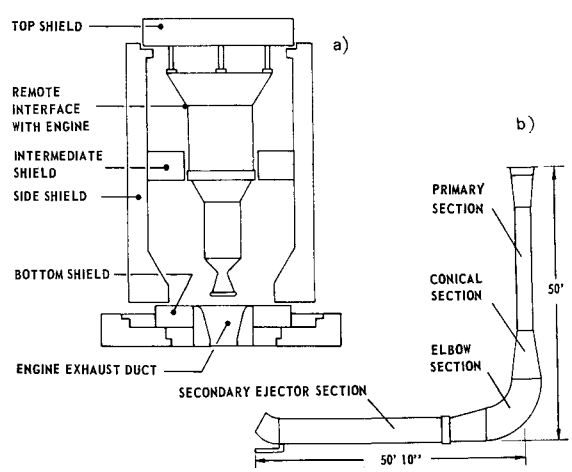

Fig. 1 a) Engine test compartment; b) NES duct.

Presented as Paper 69-325 at the AIAA 3rd Flight Test, Simulation, and Support Conference, Houston, Texas, March 10–12, 1969; submitted March 24, 1969; revision received August 25, 1969.

* Senior Engineering Specialist, Systems Analysis Section. Member AIAA.
† Senior Engineering Specialist, Thermodynamics Section.
‡ Assistant Manager, Systems Department. Member AIAA.

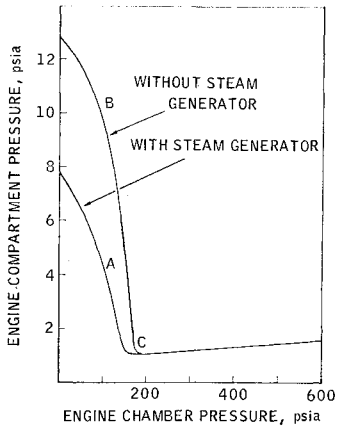

Fig. 2 Predicted performance of ETS-1.

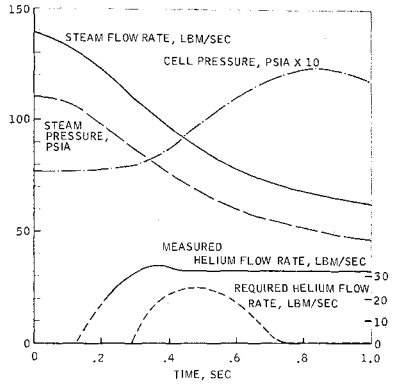

Fig. 4 Estimated and experimental results from helium flow tests.

mined. To estimate the steam (and thus air) needed to repressurize the cell, the mixed-mean properties of the fluid mixture were calculated by assuming perfect mixing.

The analytical results were compared with developmental test data in the full-scale duct with cold N_2 used as the primary fluid, and agreement was good. Specifically, the analysis predicted air intrusion for all runs where air backflow was detected by the oxygen analyzers. For example, Fig. 3 shows that air will enter the cell during the shutdown of the SGS (simulated malfunction) for a typical run.

Equation (1) indicates that air intrusion can be prevented either by decreasing dP_1/dt or increasing W_p so that the left side of Eq. (1) is always lower than the right side. Two corresponding systems for preventing air backflow that were considered are an on-line steam accumulator and a purge gas system. For the former, the interrelationship between the steam decay rate dP_s/dt and the cell repressurization rate dP_1/dt was established from full-scale tests with cold nitrogen gas as the primary fluid: $dP_1/dt = -0.116\ dP_s/dt$. The rates were assumed to occur under quasi-steady-state conditions, and dP_s/dt was calculated by assuming adiabatic venting of steam through a sonic nozzle. The amount of steam required was calculated by using mixed-mean properties, and a 2000-ft^3 accumulator was found to be adequate. The second approach would require 30 lbm/sec of helium at ambient conditions for a typical experimental NERVA engine test. Such a scheme is expensive and lowers the altitude-simulation capability of the exhaust system, because the equilibrium cell pressure is higher. However, if a control system can be designed that detects a malfunction in the SGS and introduces a sufficient quantity of a purge gas within 0.3 sec of malfunction through a fast-acting valve, air intrusion can be prevented (see Fig. 4). Since this method offered advantages over the others, it was selected as the safety system during the operation of the NES duct with the experimental NERVA engine.

To verify the soundness of the analytical model and the operational capability of the control system to detect a malfunction in the SGS, tests were conducted by using the full-scale hardware under simulated malfunction conditions. The measured He flow rate is shown in Fig. 4. To verify the analytical calculations, high-speed motion pictures of the gas flow at the duct exit were taken, and flow of the exhaust gases at the duct exit was monitored by closed-circuit TV cameras. Aerodynamic tufts (a rake of thin metal ribbons) were attached to the exit plane of the duct, and four oxygen analyzers were placed at various locations within the ETC. None of these indicated air backflow.

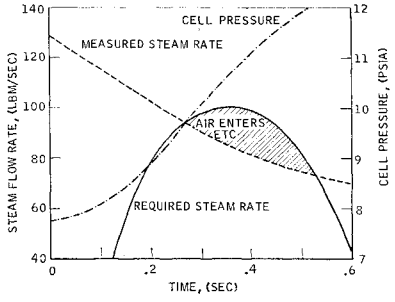

Fig. 3 Nitrogen flow test results—run 3.

Overpressurization

Analytical techniques based on linear network theory are used to predict the frequency and amplitude of pressure oscillations with a two-node network with an equivalent R-L-C network. Gas in a short open tube of length L and cross-sectional area A (see Fig. 5a) behaves as an incompressible (rigid) body, so that continuity is achieved. Therefore, Newton's second law may be written

$$\Sigma F = (P_1 - P_2)A = m\dot{U}/g_c = (L/g_c)d\dot{m}/dt \qquad (2)$$

Fluid inductance is defined as

$$\Delta P = \bar{L}d\dot{m}/dt, \text{ or } \bar{L} = L/Ag_c \qquad (3)$$

The gas contained in a short, closed-end tube (Fig. 5b) behaves as a spring, with flow rate related to the change in pressure by

$$\dot{m} = (\rho AL/K)(dP/dt) \qquad (4)$$

The compliance is defined as

$$C \equiv \int \dot{m}dt/\Delta P, \text{ or } C = \rho AL/K \qquad (5)$$

The resistance for laminar flow and turbulent flow may be stated, respectively,

$$\Delta P = 8\pi\mu L\dot{m}/A^2\rho = \dot{m}R \qquad (6)$$

$$R = m(fL/D + K_e + K_c)/2g_c \qquad (7)$$

Figure 5d shows an idealized model of the ETS-1 duct that is more practical to analyze, whereas Fig. 5e shows a schematic of the duct. The sum of the pressure losses (inertial, re-

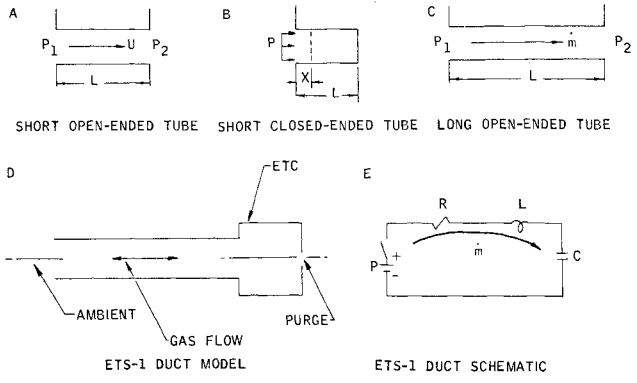

Fig. 5 Representation of the lumped parameter technique for the ETS-1 duct.

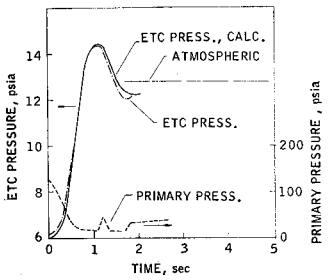

Fig. 6 Predicted and experimental nitrogen test results for ETS-1.

sistance and capacitive) is equated to the line terminal-pressure differences;

$$L\dot{m}/dt + R\dot{m} + 1/C\int\dot{m}/dt = P - \gamma \quad (8)$$

Clement and Johnson[1] obtain for the cell pressure the expression

$$P = \gamma + (P\infty - \gamma)[1 - e^{\alpha\sim t}(\cos\omega_t + \alpha/\omega \sin\omega_t)] \quad (9)$$

where

$$A = R/2\bar{L},\ \omega = 1/\bar{L}C - R^2/4\bar{L}^2 \quad (10)$$

In applying this method, the equivalent resistance of the duct is taken from the calculations of mass flow and pressure loss. The entrance and exit loss coefficients, K_e and K_c, respectively, are taken from London and Kays.[2]

For a $\frac{1}{8}$-scale program conducted at the Aerojet-General Corporation's Azusa Facility, the duct constants were calculated to be: α = 14.28 rad/sec, ω = 49.4 rad/sec. The ramp time required for the analysis was determined from gas pressure measurements either in the ejector manifold or the engine chamber. For the 10 tests, the average deviation from test data were 0.16 psi (8%) over-pressure and 0.036 sec (6%) in response time.

Five full-scale tests with N_2 without SGS were evaluated similarly. The test involved the sudden shutoff of the primary flow. The resistance of the duct with end effects included is R = 0.792 lbf-sec/lb-ft². The compliance is determined from the average change in pressure which results from the addition of 1 lb of gas, or by use of Eq. (5). With ETC volume = 5925 ft³, for gaseous N_2 at 520°R, the compliance (ETC + duct) is C = 0.2065 lb-ft²/lbf. Then with L = 0.2767 sec²/ft² (see Fig. 6), Eq. (11) gives (for A = 12.4 ft², L = 110 ft) α = 1.43 rad/sec, and ω = 3.93 rad/sec. The analysis shows (See Fig. 6) that ETC repressurizes to a maximum of 14.5 psia which is 1.7 psi higher than the ambient pressure of 12.8 psia at NRDS, reaching this pressure level 1.1 after the primary flow starts to decrease. The initial surge is followed by a series of pressure oscillations that are effectively damped in 5.5 sec (not shown).

The ETS-1 was also tested with He to provide a more realistic evaluation than was obtained from tests with N_2. The SGS flow was cut off as rapidly as practicable by shutting down the steam generators simultaneously. The test results are shown on Fig. 7. From the steam flow decay rate and the purge gas flow rate predicted ETC pressure is also shown on Fig. 7. It should be noted that the predicted ETC pressure peak occurs approximately the same time and has the same magnitude as the measured value.

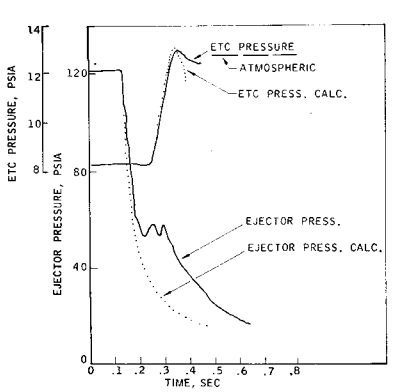

Fig. 7 Predicted and experimental helium test results for ETS-1.

In conclusion, the results of the analytical model agree well with the experimental data. The analytical predictions were confirmed by both visual observation and by using oxygen analyzers. The model can be used efficiently to modify either the design or the operating conditions for over-all system improvement.

References

[1] Clement, P. R. and Johnson, W. C., *Electrical Engineering*, McGraw-Hill, 1960, p. 265.

[2] Kays, W. M. and London, A. L., *Compact Heat Exchangers*, National Press, Palo Alto, Calif., 1955.

Gravity-Gradient Capture and Stability in an Eccentric Orbit

D. K. ANAND,* J. M. WHISNANT,† V. L. PISACANE,‡ AND M. STURMANIS†

The Johns Hopkins University, Silver Spring, Md.

Introduction

GRAVITY-GRADIENT stabilization of artificial satellites in near-circular orbits has been well demonstrated in the past. In this Note the capture and stabilization of a satellite in a highly eccentric orbit is considered. The satellite under consideration is Lidos, whose purpose is to yield geodetic information. It has an unsymmetrical inertia ellipsoid, four solar paddles arranged in a windmill fashion, a self-erecting boom with end mass, permeable rods for hysteretic damping and a dipole magnet for performing inversion maneuvers in case the satellite is initially captured in the undesired mode.

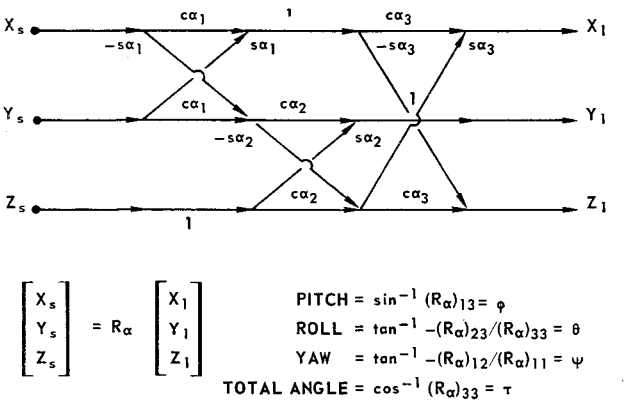

Fig. 1 Coordinate transformation and angle representation.

Presented as Paper 69-921 at the AIAA/AAS Astrodynamics Conference, Princeton, N.J., August 20–22, 1969; submitted August 12, 1969; revision received September 10, 1969. This work was done under Navy Contract NOw-62-0604-c.

* Senior Staff, Space Research and Analysis Branch, Applied Physics Laboratory; also Associate Professor of Mechanical Engineering, University of Maryland. Member AIAA.

† Associate Mathematician, Space Research and Analysis Branch, Applied Physics Laboratory.

‡ Supervisor, Theory Project, Space Research and Analysis Branch, Applied Physics Laboratory. Member AIAA.